



Cite this: DOI: 10.1039/c4tc02879a

Simultaneous modification of *N*-alkyl chains on cyclometalated and ancillary ligands of cationic iridium(III) complexes towards efficient piezochromic luminescence properties†

Yi Han,^a Hong-Tao Cao,^a Hai-Zhu Sun,^a Guo-Gang Shan,^{*a} Yong Wu,^a
Zhong-Min Su^{*a} and Yi Liao^{*b}

In this study, we have designed and synthesized a series of multifunctional cationic iridium(III) complexes with different lengths of *N*-alkyl chains on 2-phenyl-1*H*-benzimidazole-based cyclometalated ligands and phenyl-pyridine type ancillary ligands. The photophysical properties of each complex have been investigated in detail and also ascertained by comprehensive density functional theory calculations. Despite showing negligible influence on their emission spectra and excited-state characteristics in solution, altering the *N*-alkyl chain length can efficiently modify their photophysical properties in the solid state. All complexes exhibit fascinating visible piezochromic luminescence (PCL) behaviour. Most interestingly, these iridium(III)-based luminophores with longer *N*-alkyl chains display significant emission colour changes and unique reversible features by mechanical grinding and solvent fuming. The powder X-ray diffraction (PXRD), ¹H NMR and MALDI-TOF/TOF mass spectrometry data demonstrate that the phase transitions between crystalline and amorphous states are crucial to the present piezochromism. Moreover, with the merit of high quantum efficiency in aggregate states, the studied iridium(III) complex can serve as an efficient sensor for the sensitive and selective detection of the explosive, 2,4,6-trinitrophenol (TNP).

Received 15th December 2014
Accepted 13th January 2015

DOI: 10.1039/c4tc02879a

www.rsc.org/MaterialsC

Introduction

Stimuli-responsive luminescent materials presenting colour changes under external stimuli such as heat, light, electricity, pH and mechanical forces are considered as “smart” materials.¹ Such materials have attracted extensive attention due to their academic importance and promising applications.² Among them, piezochromic luminescent (PCL) materials showing dynamic optical switching properties under mechanical stimulus environments possess potential applications in the field of optoelectronics, such as optical recordings, sensors, memory devices and switches.³ A commonly pursued approach for changing their emission characteristics is to control the molecular stacking between stable crystalline states and metastable amorphous states without the use of chemical reactions.⁴ Recently, a number of materials displaying PCL behavior have been reported, including organic and inorganic complexes,

liquid crystals, polymers as well as metal–organic frameworks.⁵ Nevertheless, organometallic complexes with PCL behaviour are rarely reported, although they exhibit preferable photophysical properties. Moreover, the lack of adequate reports on their structure–property relationships has made the controllable design and synthesis of PCL materials difficult. Therefore, it is still a great challenge to develop a new series of organometallic complexes with excellent PCL features.

Organometallic iridium(III) complexes have attracted much interest owing to their excellent photophysical and photochemical properties, *i.e.*, high quantum efficiency, as well as tunable emission wavelengths.⁶ In recent years, Huang *et al.*,⁷ Talarico *et al.*,⁸ and our group⁹ have developed a set of iridium(III) complexes with intriguing PCL behaviour. Iridium(III)-based rewritable data records and storage devices have been achieved, which will open up a new avenue for the development of multifunctional iridium(III) complexes in the future.⁷ Most recently, introducing different alkyl groups into PCL materials has proven to be effective in constructing novel PCL dyes and investigating the relationship between the molecular structures and PCL behaviours.^{4b,10} Taking these into consideration, we have designed and synthesized two series of iridium(III) complexes with different *N*-alkyl chains on cyclometalated or ancillary ligands, respectively.¹¹ The results demonstrate that

^aInstitute of Functional Material Chemistry, Faculty of Chemistry, Northeast Normal University, Changchun, 130024 Jilin, People's Republic of China. E-mail: shangg187@nenu.edu.cn; zmsu@nenu.edu.cn

^bDepartment of Chemistry, Capital Normal University, Beijing, People's Republic of China. E-mail: liaoy271@nenu.edu.cn

† Electronic supplementary information (ESI) available: Computational details and corresponding photophysical results. See DOI: 10.1039/c4tc02879a

such chromophores exhibit the opposite PCL effect. For example, the complexes with shorter *N*-alkyl chains on the ancillary ligand display more significant PCL features but more hindered reversibility. Nevertheless, the ones containing shorter *N*-alkyl chains on the cyclometalated ligand show insignificant PCL properties but better reversibility. It is generally known that both significant PCL features and reversibility are highly required for real-world practical applications. Therefore, the development of new iridium(III)-based phosphors with efficient PCL behaviour and excellent reversibility is strikingly desirable. Based on our previous studies, we speculate that such materials can be constructed by simultaneously modifying both ligands of iridium(III) complexes with *N*-alkyl chains.

Keeping this in mind, we herein report the design and synthesis of a series of iridium(III) complexes with the same *N*-alkyl chains on cyclometalated and ancillary ligands, as shown in Scheme 1. All complexes exhibit obvious piezochromism with chain length-dependency. More importantly, complex 4 with the longest *N*-alkyl chain length simultaneously showed the most significant PCL properties and reversibility when compared to others. Upon fuming with organic solvents, its emission colour can recover to the original one and this process can be reiterated several times without any deterioration. The obtained results clearly demonstrate that the present mechanochromic behaviour is attributed to the crystal-to-amorphous phase transformation. Additionally, all synthesized complexes are efficient luminophores in their solid states. With the merit of high luminescence efficiency, complex 4 can also be used as an effective chemosensor for sensitive and selective detection of nitroaromatic explosives on the ppm scale.

Experimental section

General information and materials

All reagents and solvents employed were commercially available and used as received without further purification. Solvents for syntheses were freshly distilled over appropriate drying reagents. All experiments were performed under a nitrogen atmosphere by using standard Schlenk techniques. NMR spectra were recorded on a Bruker Avance 500 MHz (^1H : 500 MHz, ^{19}F : 470 MHz). The molecular weights of the complexes were measured by using electrospray-ionization mass spectroscopy (MS) and matrix-assisted laser desorption-ionization time-of-flight (MALDI-TOF) mass spectrometry. The emission spectra were recorded by using a F-4600 FL spectrophotometer. The excited-state lifetimes were measured on a transient spectrofluorometer (Edinburgh FLS920) with a time-correlated single-photo counting technique. Powder X-ray diffraction (PXRD) patterns of the samples were collected on a Rigaku Dmax 2000.

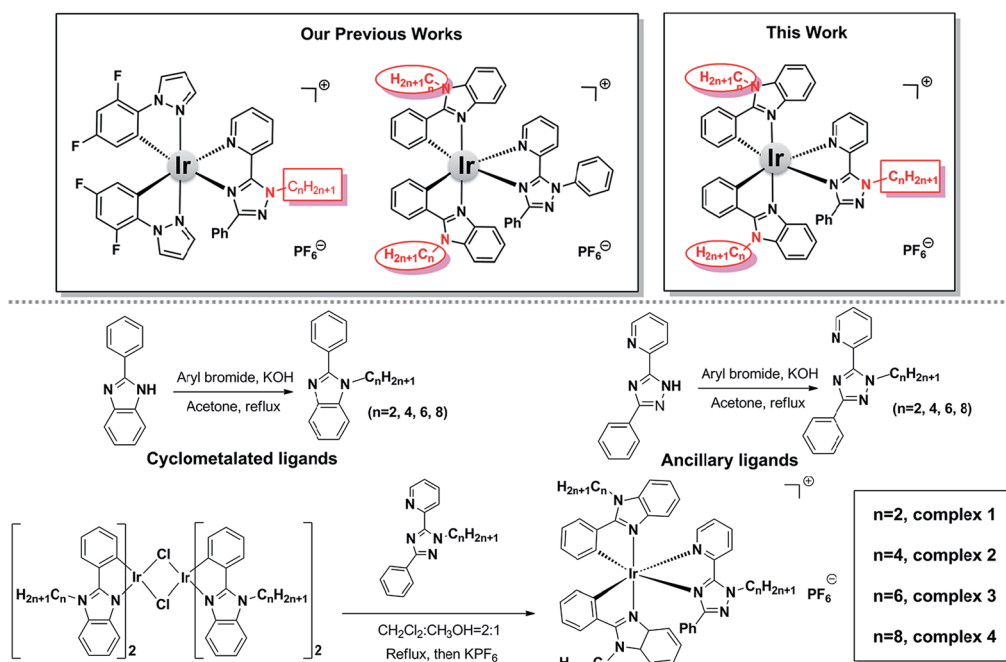
Synthesis

Synthesis of the cyclometalated and ancillary ligands.

Scheme 1 depicts the synthetic routes to the cyclometalated and ancillary ligands. As shown in Scheme 1, the ligands used in this work can be easily synthesized by the condensation of 2-phenyl-1*H*-benzo[*d*]imidazole or 2-phenyl-1*H*-benzo[*d*]imidazole with corresponding aryl bromide in acetone solvent in the presence of KOH.^{9b,11b}

Synthesis of the ancillary ligands

2-(1-Ethyl-3-phenyl-1*H*-1,2,4-triazol-5-yl)pyridine (*Ethtaz*). The precursor 2-(3-phenyl-1*H*-1,2,4-triazol-5-yl)pyridine (1.11 g, 5.00



Scheme 1 Chemical structures of the reported Ir(III)-based phosphors and synthesis of the ligands and the iridium(III) complexes studied in this work.

mmol) was synthesized by a previously reported procedure.^{11a,12} Under a nitrogen atmosphere, the precursor was dissolved in acetone. An equivalent amount of KOH was added and the mixture was stirred for 30 min. Then, bromoethane (0.65 g, 6.00 mmol) was added into the reaction mixture and the mixture was heated to reflux overnight. After cooling to room temperature, the mixture was quenched with ice water and then extracted with dichloromethane. The organic layer was dried with Na₂SO₄ and the solvent was removed. The obtained residues were purified by column chromatography on silica gel with ethyl acetate/petroleum ether (v/v = 1 : 2) as the eluent to yield a light-yellow oil (60%). ¹H NMR (500 MHz, CDCl₃, ppm): δ 8.64–8.65 (m, 1H), 8.30 (d, *J* = 8.0 Hz, 1H), 8.17–8.19 (m, 2H), 7.79–7.81 (m, 1H), 7.44–7.46 (m, 2H), 7.38–7.40 (m, 1H), 7.28–7.30 (m, 1H), 4.87 (t, *J* = 8.0 Hz, 2H), 1.52–1.55 (m, 3H). The related ancillary ligands (Buttaz, Hextaz, and Octtaz) were prepared using similar procedures.

2-(1-Butyl-3-phenyl-1H-1,2,4-triazol-5-yl)pyridine (Buttaz).

¹H NMR (500 MHz, CDCl₃, ppm): δ 8.66–8.67 (m, 1H), 8.31 (d, *J* = 8.0 Hz, 1H), 8.16–8.18 (m, 2H), 7.81–7.84 (m, 1H), 7.43–7.46 (m, 2H), 7.37–7.40 (m, 1H), 7.31–7.34 (m, 1H), 4.85 (t, *J* = 7.5 Hz, 2H), 1.90–1.96 (m, 2H), 1.37–1.42 (m, 2H), 0.93 (t, *J* = 7.5 Hz, 3H).

2-(1-Hexyl-3-phenyl-1H-1,2,4-triazol-5-yl)pyridine (Hextaz).

¹H NMR (500 MHz, CDCl₃, ppm): δ 8.66–8.67 (m, 1H), 8.30 (d, *J* = 8.0 Hz, 1H), 8.16–8.18 (m, 2H), 7.81–7.84 (m, 1H), 7.43–7.46 (m, 2H), 7.37–7.40 (m, 1H), 7.31–7.34 (m, 1H), 4.83 (t, *J* = 7.5 Hz, 2H), 1.92–1.96 (m, 2H), 1.25–1.38 (m, 6H), 0.86 (t, *J* = 7.5 Hz, 3H).

2-(1-Octyl-3-phenyl-1H-1,2,4-triazol-5-yl)pyridine (Octtaz).

¹H NMR (500 MHz, CDCl₃, ppm): δ 8.66–8.67 (m, 1H), 8.31 (d, *J* = 8 Hz, 1H), 8.16–8.18 (m, 2H), 7.81–7.85 (m, 1H), 7.43–7.46 (m, 2H), 7.37–7.40 (m, 1H), 7.31–7.34 (m, 1H), 4.83 (t, *J* = 7.5 Hz, 2H), 1.92–1.96 (m, 2H), 1.22–1.37 (m, 10H), 0.86 (t, *J* = 7.5 Hz, 3H).

Synthesis of the cyclometalated ligands

Ethyl-2-phenyl-1H-benzo[d]imidazole (Eebd). ¹H NMR (500 MHz, CDCl₃, ppm): δ 7.84–7.86 (m, 1H), 7.73–7.74 (m, 2H), 7.52–7.54 (m, 3H), 7.43 (t, *J* = 4.5 Hz, 1H), 7.31–7.33 (m, 2H), 4.26–4.29 (m, 2H), 1.45 (t, *J* = 7 Hz, 3H).

Butyl-2-phenyl-1H-benzo[d]imidazole (Bebd). ¹H NMR (500 MHz, CDCl₃, ppm): δ 7.84–7.86 (m, 1H), 7.72–7.74 (m, 2H), 7.52–7.54 (m, 3H), 7.42 (t, *J* = 4.5 Hz, 1H), 7.31–7.33 (m, 2H), 4.21 (t, *J* = 7.5 Hz, 2H), 1.79 (t, *J* = 7.5 Hz, 2H), 1.25–1.29 (m, 2H), 0.84 (t, *J* = 7.5 Hz, 3H).

Hexyl-2-phenyl-1H-benzo[d]imidazole (Hebd). ¹H NMR (500 MHz, CDCl₃, ppm): δ 7.84–7.86 (m, 1H), 7.71–7.73 (m, 2H), 7.51–7.54 (m, 3H), 7.40 (t, *J* = 4.5 Hz, 1H), 7.29–7.31 (m, 2H), 4.19 (t, *J* = 7.5 Hz, 2H), 1.79 (t, *J* = 7.0 Hz, 2H), 1.21–1.25 (m, 6H), 0.84 (t, *J* = 6.5 Hz, 3H).

Octyl-2-phenyl-1H-benzo[d]imidazole (Oebd). ¹H NMR (500 MHz, CDCl₃, ppm): δ 7.84–7.86 (m, 1H), 7.71–7.72 (m, 2H), 7.50–7.52 (m, 3H), 7.41 (t, *J* = 3.0 Hz, 1H), 7.30–7.32 (m, 2H), 4.20 (t, *J* = 7.5 Hz, 2H), 1.79 (t, *J* = 7 Hz, 2H), 1.19–1.26 (m, 10H), 0.84 (t, *J* = 6.5 Hz, 3H).

Synthesis of the chloro-bridged dimer. The organo-metallated dimer [Ir(Eebd)₂Cl]₂ was synthesized by the reaction of IrCl₃·3H₂O (0.51 g, 1.43 mmol) with ethyl-2-phenyl-1H-benzo[d]imidazole (Eebd 0.66 g, 3.15 mmol) in a 2-ethoxyethanol and

water mixture (v/v = 3 : 1, 32 mL) for 24 h. The mixture was treated with water (30 mL) to induce precipitation of the off-white solid. The product was filtered and washed with diethyl ether followed by with ethanol, and dried (yield: 74%). Other chloride-bridged complexes, [Ir(Bebd)₂Cl]₂, [Ir(Hebd)₂Cl]₂, and [Ir(Oebd)₂Cl]₂, were synthesized using a method similar to that for [Ir(Eebd)₂Cl]₂. The chloro-bridged dimers were used in the subsequent reactions without further purification.

Synthesis of the complexes

Synthesis and characterization of complex 1. A solution of ligand Ethtaz (0.21 g, 0.63 mmol) and the chloro-bridged dimer [Ir(Eebd)₂Cl]₂ (0.56 g, 0.30 mmol) in a solvent mixture of methanol (15 mL) and dichloromethane (30 mL) was refluxed for 24 h in the dark. After cooling to room temperature, the mixture was filtered, and then an excess of solid KPF₆ was added and stirred for another 0.5 h at room temperature. The solvent was removed under reduced pressure. The crude product was purified by silica gel column chromatography using dichloromethane/ethyl acetate (v/v = 5 : 1) and the resulting powders were recrystallized from a dichloromethane and petroleum ether mixture to give complex 1 as a light-yellow solid (yield 58%). ¹H NMR (500 MHz, d₆-DMSO, ppm): δ 8.60 (d, *J* = 8.0 Hz, 1H), 8.34 (d, *J* = 8.0 Hz, 1H), 7.98 (d, *J* = 8.0 Hz, 1H), 7.88 (d, *J* = 8.5 Hz, 1H), 7.82 (d, *J* = 8.0 Hz, 1H), 7.72–7.79 (m, 2H), 7.38 (t, *J* = 7.5 Hz, 1H), 7.29–7.32 (m, 2H), 7.18–7.21 (m, 1H), 7.12–7.14 (m, 3H), 7.05–7.08 (m, 1H), 6.87 (t, *J* = 8.0 Hz, 1H), 6.83–6.86 (m, 2H), 6.76–6.79 (m, 2H), 6.70 (t, *J* = 7.5 Hz, 1H), 6.60 (t, *J* = 7.5 Hz, 1H), 6.26 (d, *J* = 8.0 Hz, 1H), 5.94 (d, *J* = 7.5 Hz, 1H), 5.68 (d, *J* = 8.0 Hz, 1H), 4.77–4.95 (m, 4H), 4.65–4.68 (m, 1H), 4.55–4.58 (m, 1H), 1.51 (t, *J* = 7.5 Hz, 3H), 1.22–1.31 (m, 6H). ¹⁹F NMR (470 MHz, d₆-DMSO, ppm): –67.35 (d, *J* = 711.11 Hz, 6F). MS (MALDI-TOF): *m/z* 885.3 (M – PF₆).

Synthesis and characterization of complex 2. Light-yellow solid, (yield 62%). ¹H NMR (500 MHz, d₆-DMSO, ppm): δ 8.62 (d, *J* = 8.0 Hz, 1H), 8.35 (d, *J* = 8.0 Hz, 1H), 7.98 (d, *J* = 8.0 Hz, 2H), 7.89 (d, *J* = 8.5 Hz, 1H), 7.74–7.79 (m, 2H), 7.38 (t, *J* = 8.0 Hz, 1H), 7.24–7.30 (m, 2H), 7.13–7.19 (m, 4H), 7.05–7.08 (m, 1H), 6.96 (t, *J* = 8.0 Hz, 1H), 6.86–6.88 (m, 3H), 6.74–6.75 (m, 1H), 6.68 (t, *J* = 8.0 Hz, 1H), 6.59 (t, *J* = 7.5 Hz, 1H), 6.17 (d, *J* = 8.0 Hz, 1H), 5.99 (d, *J* = 7.5 Hz, 1H), 5.64 (d, *J* = 8.0 Hz, 1H), 4.88–4.97 (m, 3H), 4.51–4.73 (m, 3H), 1.92 (t, *J* = 7.5 Hz, 2H), 1.19–1.69 (m, 10H), 0.68–0.93 (m, 6H), 0.66–0.68 (m, 3H), 1.19–1.69 (m, 1H). ¹⁹F NMR (470 MHz, d₆-DMSO, ppm): –67.35 (d, *J* = 711.11 Hz, 6F). MS (MALDI-TOF): *m/z* 969.4 (M – PF₆).

Synthesis and characterization of complex 3. Light-green solid, (yield 69%). ¹H NMR (500 MHz, d₆-DMSO, ppm): δ 8.63 (d, *J* = 8.0 Hz, 1H), 8.34 (t, *J* = 8.0 Hz, 1H), 7.98 (d, *J* = 8.0 Hz, 2H), 7.89 (t, *J* = 8.5 Hz, 1H), 7.73–7.79 (m, 2H), 7.38 (t, *J* = 8.0 Hz, 1H), 7.23–7.28 (m, 2H), 7.12–7.17 (m, 4H), 7.04–7.08 (m, 1H), 6.96 (t, *J* = 8.0 Hz, 1H), 6.84–6.89 (m, 3H), 6.69–6.74 (m, 2H), 6.59 (t, *J* = 7.5 Hz, 1H), 6.17 (d, *J* = 7.5 Hz, 1H), 6.00 (d, *J* = 7.5 Hz, 1H), 5.64 (d, *J* = 8.0 Hz, 1H), 4.87–4.99 (m, 3H), 4.51–4.69 (m, 3H), 1.91–1.97 (m, 2H), 1.50–1.70 (m, 4H), 0.97–1.39 (m, 17H), 0.75–0.86 (m, 10H). ¹⁹F NMR (470 MHz, d₆-DMSO, ppm): –67.35 (d, *J* = 711.11 Hz, 6F). MS (MALDI-TOF): *m/z* 1053.5 (M – PF₆).

Synthesis and characterization of complex 4. Light-green solid (yield 74%). ¹H NMR (500 MHz, d₆-DMSO, ppm): δ 8.63 (d,

$J = 7.5$ Hz, 1H), 8.34 (t, $J = 7.5$ Hz, 1H), 7.95–7.99 (m, 2H), 7.89–7.91 (m, 1H), 7.77 (d, $J = 8.0$ Hz, 1H), 7.73 (d, $J = 7.5$ Hz, 1H), 7.38 (t, $J = 7.5$ Hz, 1H), 7.22–7.28 (m, 2H), 7.12–7.19 (m, 4H), 7.04–7.07 (m, 1H), 6.94 (t, $J = 8.0$ Hz, 1H), 6.83–6.89 (m, 3H), 6.74 (t, $J = 7.5$ Hz, 1H), 6.68 (t, $J = 7.5$ Hz, 1H), 6.58 (t, $J = 7.5$ Hz, 1H), 6.16 (d, $J = 7.0$ Hz, 1H), 6.00 (d, $J = 7.5$ Hz, 1H), 5.62 (d, $J = 8.0$ Hz, 1H), 4.90–5.00 (m, 3H), 4.51–4.68 (m, 3H), 1.92–1.95 (m, 2H), 1.49–1.70 (m, 4H), 0.97–1.37 (m, 29H), 0.69–0.87 (m, 10H). ^{19}F NMR (470 MHz, d_6 -DMSO, ppm): -67.35 (d, $J = 711.11$ Hz, 6F). MS (MALDI-TOF): m/z 1137.6 ($M - \text{PF}_6$).

Theoretical calculations

All calculations on the ground and excited electronic states of the complexes were carried out at the PBE0 level using the Gaussian 09 software package¹³ together with 6-31G* basis sets for C, H, N atoms and the LANL2DZ for the Ir atom. An effective core potential (ECP) replaces the inner core electrons of iridium leaving the outer core $(5s)^2(5p)^6$ electrons and the $(5d)^6$ valence electrons of Ir(III). The geometry of the lowest-lying triplet (T_1) states was fully optimized and calculated at the spin-unrestricted UPBE0 level with a spin multiplicity of 3. All expectation values calculated for S^2 were smaller than 2.05.

Results and discussion

Photophysical properties in solution and solid state

Fig. 1 shows the emission spectra of complexes **1–4** in CH_3CN solution at room temperature (RT) and 77 K, and the relevant data are summarized in Table S1.† The sub-microsecond ranges of emissive lifetimes clearly demonstrate their phosphorescence emission nature.¹⁴ It is well known that three excited states can contribute to the observation of light emission for cationic iridium(III) complexes, namely spin-forbidden metal-to-ligand charge transfer ($^3\text{MLCT}$), ligand-to-ligand charge transfer ($^3\text{LLCT}$) and ligand-centered ($\text{LC } ^3\pi-\pi^*$) characters.¹⁵ As shown in Fig. 1, at room temperature, complexes **1–4** exhibit broad and featureless emission spectra in solution, indicating that their emissions mainly originated from $^3\text{MLCT}$ and/or $^3\text{LLCT}$ states rather than from $\text{LC } ^3\pi-\pi^*$, since the emissions from $\text{LC } ^3\pi-\pi^*$ states always are vibronically structured.^{6c} After cooling the solution to 77 K, all complexes display largely blue-shifted

emission spectra compared to those at RT (Fig. 1). It is noteworthy that although different alkyl chains are attached to these complexes, they display a similar emission pattern at RT and 77 K. These results suggest that altering the *N*-alkyl chains on both ligands shows a negligible impact on their phosphorescence spectra as well as excited-state characteristics in solution. To verify this issue, the density functional theory (DFT) and time-dependent DFT (TD-DFT) calculations have been performed on them to ascertain the nature of their excited states. As depicted in Fig. 2, the highest-occupied molecular orbital (HOMO) of complex **1** mainly resides on the benzimidazole group of the cyclometalated ligands and the iridium ion, while the lowest unoccupied molecular orbital (LUMO) primarily delocalizes over the pyridine and 1,2,4-triazole moieties of the ancillary ligands. Complexes **2–4** show almost identical HOMO and LUMO distributions (see Fig. S1, ESI†). Clearly, the *N*-alkyl chains in **1–4** do not contribute to either the HOMOs or LUMOs. The TD-DFT data show that the lowest-lying triplet (T_1) states of the complexes mainly originate from the excitation of HOMO \rightarrow LUMO (see Table S2, ESI†). Therefore, the T_1 states have predominantly mixed $^3\text{MLCT}$ and $^3\text{LLCT}$ characteristics. The charge transfer nature of the emitting triplets is in agreement with the experimental emission spectra. In addition, the unpaired-electron spin density distribution perfectly matches the topology of the HOMO \rightarrow LUMO excitation from which the T_1 excited-states originate (see Fig. 2). These results further confirm that the mixed $^3\text{MLCT}$ and $^3\text{LLCT}$ excited-state characters are attributed to their T_1 states and the different *N*-alkyl chains have little effect on their emission in solutions.

Despite **1–4** exhibit identical emission spectra as well as luminescent colours in solution, their solid-state emissions are obviously different. They display bright luminescence with emission colours ranging from yellow (542 nm for **1**) to green (513 nm for **4**), respectively. The relevant solid-state emission data are given in Table 1. It is generally recognized that the solid-state emission properties of luminophores strongly depend on the molecular arrangement of motifs and intermolecular interactions.¹⁶ As a result, we conjecture that adjusting *N*-alkyl chains attached to iridium(III) complexes can induce different molecular packing and hence emission colours in solid-states. Longer *N*-alkyl chains might impede close packing, which results in loose molecular packing and blue-shifted emission spectra. Similar to previous reports, simultaneously modifying the *N*-alkyl chain on both ligands of cationic

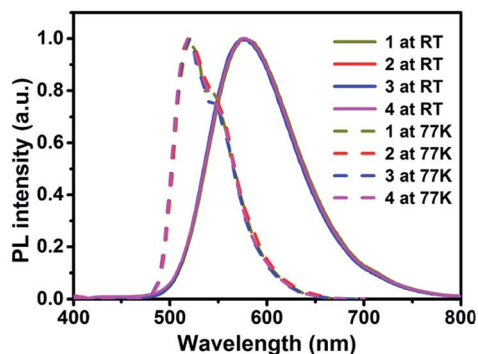


Fig. 1 Emission spectra of complexes **1–4** in CH_3CN (1×10^{-5} M) at 298 and 77 K.

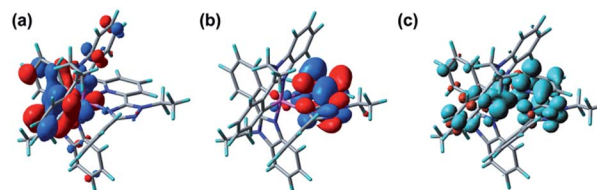


Fig. 2 Electronic density contours calculated for the HOMO (a) and the LUMO (b) of complex **1**. (c) Spin density distribution calculated for complex **1** in the T_1 excited state.

Table 1 Emission maxima (λ , in nm) of as-synthesized, ground and fumed complexes **1–4**

Complex	$\lambda_{\text{as-synthesized}}$	λ_{ground}	$\Delta\lambda_{\text{PCL}}^a$	λ_{fumed}
1	542	563	21	548
2	536	559	23	553
3	513	550	37	544
4	519	552	33	520

$$^a \Delta\lambda_{\text{PCL}} = \lambda_{\text{ground}} - \lambda_{\text{as-synthesized}}$$

iridium(III) complexes is also an effective approach to control their photophysical properties in the solid state.¹¹

Solid-state piezochromic properties

Organic solid-state materials with tunable light-emitting behaviours have attracted much attention due to their potential applications as sensors, logicgate units, memory devices, *etc.*¹⁷ Developing such efficient materials and deeply investigating the relationship between the structure and the PCL behaviour will be valuable for further molecular design. In our previous work, the effect of *N*-alkyl chains on PCL properties was successfully accomplished, in which the *N*-alkyl chains were grafted onto either cyclometalated or ancillary ligands.¹¹ To evaluate the PCL behaviours of iridium(III) complexes studied in this work, their solid-state emissions were investigated. As shown in Fig. 3a and Table 1, the as-synthesized solid powders of complexes **1–4** emit intense yellow or green light at 542, 536, 513 and 519 nm, respectively. After grinding the original powders in agate mortars with pestles, noticeable colour changes in luminescence were observed (see Fig. 3a). Meanwhile, as visualized by the naked eye, it is found that the complexes with longer *N*-alkyl chains show more remarkable colour changes in comparison with those of the shorter ones. In other words, the grinding induced spectral shifts ($\Delta\lambda_{\text{PCL}}$, $\Delta\lambda_{\text{PCL}} = \lambda_{\text{ground}} - \lambda_{\text{as-synthesized}}$) of these iridium(III) luminophores are length-dependent, which are similar to recently reported studies. Herein, we take **1** and **4** as examples. The emission spectra of **1** and **4** in original and

ground states were studied and are shown in Fig. 3b and c. It is clear that grinding results in broadened emission spectra, showing obvious emission wavelength changes of 21 nm for **1** and 33 nm for **4**, respectively. It is generally recognized that the PCL behavior for a given luminophore is related to the arrangement of its molecular motifs as well as the intermolecular interactions. Usually, the PCL materials with weak intermolecular interactions, especially the materials functionalized with different alkyl chains, exhibit more significant PCL properties than those with stronger ones.^{10b,10c} Moreover, the existence of a large dipole moment for a D- π -A PCL dye is also favorable for significant PCL behaviors.^{3f} In this work, however, there are no D- π -A structures in the studied systems. Therefore, it is speculated that introducing long alkyl chains into both cyclometalated and ancillary ligands can weaken the intermolecular interactions more effectively. As a result, the grinding may result in more significant PCL features for iridium(III) complexes with longer alkyl chains.

As mentioned above, the cationic iridium(III) complexes possessing longer *N*-alkyl chains exhibit more efficient PCL behaviour with larger emission wavelength changes. However, it is not known whether they can also exhibit excellent colour-change reversibility triggered by external stimuli, such as grinding and solvent fuming. To check their reversibility, the grinding–fuming switching experiment was performed. All ground samples can be stable for months at room temperature. Upon treating the ground samples with ether solvent, however, the emissions are obviously blue-shifted to different degrees compared to those of ground ones (see Fig. 4, S2 and S3†). It is worth mentioning that only complex **4** exhibits more excellent reversibility, the emission of the ground sample of which can perfectly revert to the original one with the same spectral profile and emission maximum (Fig. S2 and S3†). Further grinding the fumed sample **4** leads to the orange-emitting form as seen in Fig. 4a. Its emissions can thus be reversibly switched between green-emitting and orange-emitting states several times by grinding–fuming cycles with almost no fatigue. Nevertheless, the solvent-fuming cannot entirely induce the emission colour

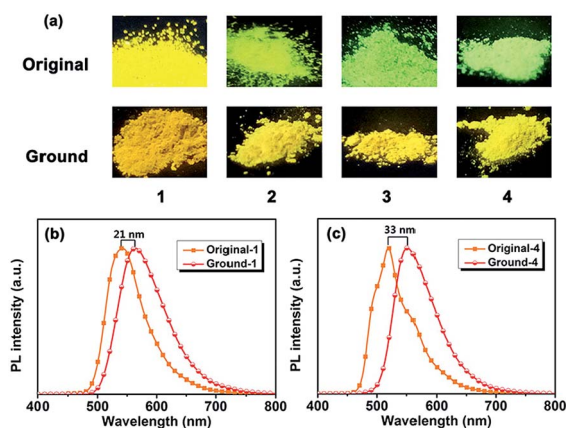


Fig. 3 (a) Photographs of complexes **1–4** taken under UV illumination (365 nm). Emission spectra of complexes **1** (b) and **4** (c) in the solid state at room temperature, respectively.

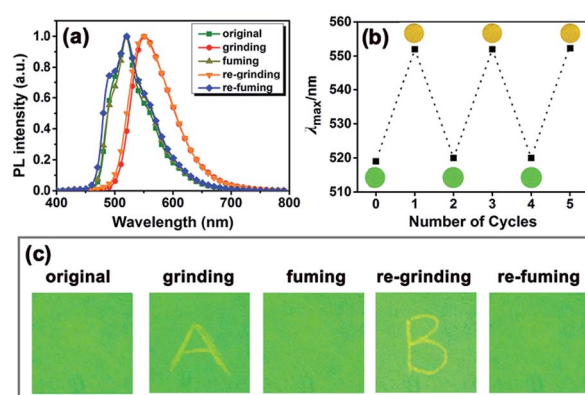


Fig. 4 (a) Emission spectra of complex **4** in various states at room temperature. (b) Maximum emission wavelength change versus repeating cycles. (c) Photographs of the reversible writing/erasing cycles using complex **4** as medium.

of ground samples 1–3 to change to their original ones. For instance, the emission colour of fumed-2 was nearly invariant with only 6 nm spectral shift with respect to its ground sample. Simultaneously attaching the long *N*-alkyl chains onto the ligands of cationic iridium(III) complexes may more effectively decrease the intermolecular interactions, which endows them with significant colour-switchable features as well as good reversibility. Hence, it is believed that introducing specific alkyl chains into cationic iridium(III) complexes to control their molecular packing is a feasible way to design and construct effective iridium(III)-based PCL materials.

It is envisioned that complex 4 can be used as an appropriate optical memory device by judicious utilization of its mechanochromism. To demonstrate its useful practical applications, a small quantity of solid powder 4 was carefully spread on a filter paper as a thin film and then subjected to solvent fuming (Fig. 4c). The strong green-emitting film is observed under 365 nm UV irradiation. The letter “A” was written on the film using a metal spatula, and a clear orange-emitting pattern “A” with large colour contrast appears, which can be readily distinguished from the bright green background. Then, upon fuming the film with diethyl ether or dropping a spot of diethyl ether onto the film, the letter “A” is immediately erased by converting the luminescent colour back to the background emission. Then, a new letter “B” with an orange-emitting colour can be re-written on this film and erased using the same method as mentioned above, demonstrating a reproducible recording–erasing process. Such fascinating features make complex 4 a promising material for recyclable optical recording and security inks.

The mechanism for the present piezochromic behaviour

Since the solid-state emission of luminophores strongly depends on the molecular structure as well as the solid packing, alteration of the molecular arrangement of motifs or phase transition between crystalline and amorphous states in response to pressure was commonly considered as the main reason for their piezochromic luminescence properties. To gain more insight into the PCL mechanism of these iridium(III) complexes, powder X-ray diffraction (PXRD) analysis was carried out, as shown in Fig. 5 and S4.† Taking complex 4 as a

representative example, the as-synthesized powder shows many sharp and intense diffraction peaks, which suggest that the solid powders obtained by column chromatography are well-ordered crystalline structures.¹⁸ In contrast, after grinding, the XRD profile shows only a few broad and weak signals, which are indicative of the transition from a crystalline to an amorphous phase.¹⁹ Similar observations are also found in other complexes (see Fig. S4†). After careful treatment of the ground samples of complex 4 with drops of diethyl ether or long time solvent-fuming, clear reflection peaks appear again, which fit well with those of the original as-prepared solid sample, demonstrating reversal from the amorphous to the crystalline phase. Although some fumed solids show different diffraction peaks from those of as-synthesized ones (1–3), it is also certain to say that the crystalline structures have formed upon fuming. Consequently, the PXRD results indicate that the emission colour changes observed upon grinding are ascribed to the phase transition between crystalline and amorphous states. It is proved that the ground samples are amorphous metastable states, which can recover to the crystalline ones under the influence of external stimuli. Once the amorphized powders are fumed by the solvent, they can spontaneously arrange themselves into a crystalline form. For complex 4, the longer alkyl chains in it will provide higher molecular mobility in comparison to others. Upon solvent fuming, the ground sample 4 can effectively recover to the original crystalline powder, which is further confirmed by similar PXRD profiles of the original and the fumed powders. This is a possible reason why complex 4 exhibits better reversibility than others.

Moreover, the time-resolved emission decay behaviours after and before grinding, and the excited-state lifetimes of complexes 1–4 in various states were studied. The lifetime data are illustrated in Table S2.† As shown in Table S2,† the weighted mean lifetimes (τ) of all ground samples are significantly different from those of the original ones. Longer lifetimes were achieved after grinding. The reported cationic iridium(III) without PCL behaviours, however, shows almost identical lifetimes under various conditions. Therefore, it can be concluded that the changes in the emission colour of these iridium(III)-based PCL materials are associated with alteration of the mode of solid-state molecular packing and/or the intermolecular interactions and hence changes in their excited-state lifetime. Their same ¹H NMR spectra in various states further confirm this point. The mechanochromic effects presented herein are thus caused by physical processes during the grinding rather than by a chemical reaction.^{3a}

Selective detection of 2,4,6-trinitrophenol TNP

Recently, detection of high explosives has become important due to homeland security, environmental and humanitarian implications.²⁰ Most high explosives are nitro-substituted organic compounds, such as 2,4,6-trinitrophenol (TNP), 2,4,6-trinitrotoluene (TNT), and 2,4-dinitrotoluene (2,4-DNT). Among them, TNP exhibits superior power to the well-known TNT and is widely used in fireworks, dyes and so on, which usually results in the contamination of soil and aquatic systems.^{20b,21} For the

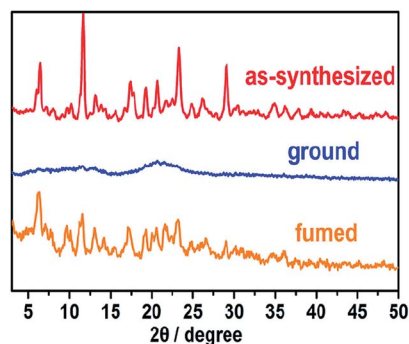


Fig. 5 PXRD patterns of complex 4 in various states.

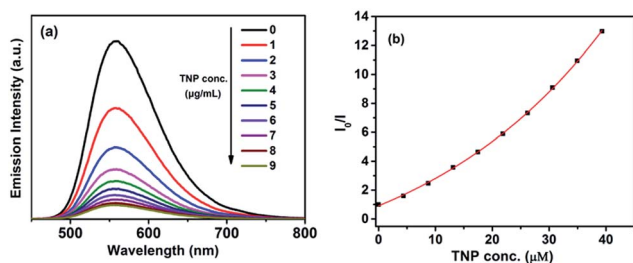


Fig. 6 (a) Photoluminescence spectra of complex **4** in acetonitrile–water ($v/v = 1 : 9$) mixtures containing different amounts of TNP. (b) Corresponding Stern–Volmer plots of TNP.

purpose of highly sensitive and selective detection of TNP in aqueous media, various chemosensors based on organic luminescent materials have been developed to date. Nevertheless, the traditional aggregation caused quenching effect in aquatic systems always results in drastically negative effects on the efficiency and sensitivity of sensors. Recent reports indicate that efficient luminophores with appropriate emission wavelengths can be used as sensitive sensors to detect TNP.²² Therefore, we herein chose complex **4** to explore its utility as a chemosensor for the detection of explosives due to its obvious aggregation-induced emission enhancement features (see Fig. S5†).

As shown in Fig. 6a, the nanoaggregates of complex **4** exhibit intense emission in the acetonitrile–water ($v/v = 1 : 9$, by volume) mixture. However, a visible emission quenching is observed with addition of a small amount of TNP into the mixtures. The luminescence intensity obviously decreases below 50% at a TNP concentration of 2 ppm. When the TNP concentration reached 9 ppm, negligible emission has been observed with a quenching efficiency of nearly 92%. The Stern–Volmer (SV) plot, as depicted in Fig. 6b, shows curves sloping upwards, which indicates that emission quenching becomes more efficient upon increasing the TNP concentration. The quenching constant is evaluated to be $1.6 \times 10^6 \text{ M}^{-1}$ by using the SV equation $(I_0/I) = K_{SV}[A] + 1$, where I and I_0 are the emission intensities with and without the quencher, respectively, K_{SV} is the quenching constant (m^{-1}), $[A]$ is the molar concentration of the quencher.²³ Such a quenching constant is higher than those of the reported fluorescent sensors for the detection of explosives, demonstrating that **4** shows a high sensitivity to TNP.²⁴ Moreover, selectivity is another key factor for a sensor. To check the sensing selectivity of complex **4**,

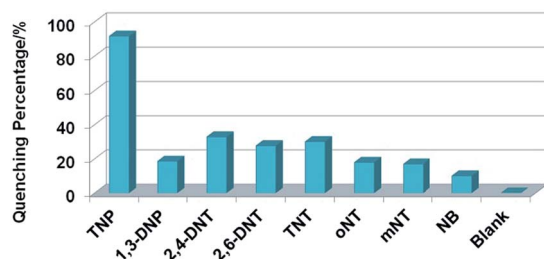


Fig. 7 Quenching percentage obtained for different analytes (9 ppm).

emission quenching experiments for other nitro aromatics, including TNT, 2,4-dinitrotoluene (2,4-DNT), nitrobenzene (NB), 2,6-dinitrotoluene (2,6-DNT), 1,3-dinitrobenzene (1,3-DNB), 2-nitrotoluene (oNT) and 3-nitrotoluene (mNT), were studied. As shown in Fig. 7, each nitroaromatic compound exhibits relatively less effect on emission quenching under the same conditions. Evidently, the emissive nanoaggregates of complex **4** display both high sensitivity and selectivity toward TNP, exploiting the potential applications of the cationic iridium(III) complexes in future. The LUMO energy of **4** is higher than those of nitroaromatic analytes, which facilitates the jump of electrons to the lower ones of analytes, leading to photo-induced electron transfer-caused (PET) emission quenching of **4** (see Fig. S6†).²⁵

Conclusions

In summary, we have designed and synthesized a series of cationic iridium(III) complexes with similar structures but different *N*-alkyl chains on both ligands. In sharp contrast to the same emission in solution, their solid-state photophysical properties exhibit *N*-alkyl chain length dependency, showing obviously blue-shifted emission upon extending their chain lengths. After grinding, each complex exhibits visible PCL. Among them, complex **4** with the longest chains features more efficient PCL properties with a larger grinding-induced emission colour change. More importantly, after treatment of ground powders with organic solvents, the emission colour of ground sample **4** can perfectly revert to its original one, but this is not the case for the other complexes. A reproducible two-colour emission writing/erasing process for **4** was thus achieved. It is believed that simultaneously introducing an appropriate *N*-alkyl chain into cationic iridium(III) complexes is a feasible design strategy for constructing effective iridium(III)-based PCL materials with good reversibility. As supported by XRD data, the present piezochromism is attributed to the transformation between crystalline and amorphous states. Inspired by intrinsic characteristics of these phosphors, a highly sensitive and selective TNP sensor based on complex **4** has also been demonstrated. The present study will provide a new insight into the design of multifunctional cationic iridium(III) complexes for optical devices and sensors in the near future.

Acknowledgements

The authors gratefully acknowledge the financial support from the National Natural Science Foundation of China (21273030, 21303012, 51203017 and 21131001), the SRFDP and RGC ERG Joint Research Program (20120043140001), the China Post-doctoral Science Foundation funded project (2013M540239 and 2014T70269), the Science and Technology Development Planning of Jilin Province (20130522167JH and 20130204025GX) and the Fundamental Research Funds for the Central Universities (12QNJJ012).

Notes and references

- 1 (a) T. Mutai, H. Satou and K. Araki, *Nat. Mater.*, 2005, **4**, 685; (b) H. Ito, M. Muromoto, S. Kurenuma, S. Ishizaka, N. Kitamura, H. Sato and T. Seki, *Nat. Commun.*, 2013, **4**, 2009; (c) Y. Ren, W. H. Kan, V. Thangadurai and T. Baumgartner, *Angew. Chem., Int. Ed.*, 2012, **51**, 3964; (d) D. P. Yan, J. Lu, J. Ma, S. H. Qin, M. Wei, D. G. Evans and X. Duan, *Angew. Chem., Int. Ed.*, 2011, **50**, 7037; (e) A. Pucci and G. Ruggeri, *J. Mater. Chem.*, 2011, **21**, 8282.
- 2 (a) K. Ariga, T. Mori and J. P. Hill, *Adv. Mater.*, 2012, **24**, 158; (b) M. M. Caruso, D. A. Davis, Q. Shen, S. A. Odom, N. R. Sottos, S. R. White and J. S. Moore, *Chem. Rev.*, 2009, **109**, 5755; (c) Y. Sagara and T. Kato, *Nat. Chem.*, 2009, **1**, 605; (d) F. Gao, Q. Liao, Z. Z. Xu, Y. H. Yue, Q. Wang, H. L. Zhang and H. B. Fu, *Angew. Chem., Int. Ed.*, 2010, **49**, 732; (e) S. C. Yu, C. C. Kwok, W. K. Chan and C. M. Che, *Adv. Mater.*, 2006, **18**, 246; (f) C. Y. K. Chan, Z. Zhao, J. W. Y. Lam, J. Liu, S. Chen, P. Lu, F. Mahtab, X. Chen, H. H. Y. Sung, H. S. Kwok, Y. Ma, I. D. Williams, K. S. Wong and B. Z. Tang, *Adv. Funct. Mater.*, 2012, **22**, 378.
- 3 (a) Z. G. Chi, X. Q. Zhang, B. J. Xu, X. Zhou, C. P. Ma, Y. Zhang, S. W. Liu and J. R. Xu, *Chem. Soc. Rev.*, 2012, **41**, 3878; (b) S. J. Toal, K. A. Jones, D. Magde and W. C. Trogler, *J. Am. Chem. Soc.*, 2005, **127**, 11661; (c) A. Kishimura, T. Yamashita, K. Yamaguchi and T. Aida, *Nat. Mater.*, 2005, **4**, 546; (d) M. Burnworth, L. Tang, J. R. Kumpfer, A. J. Duncan, F. L. Beyer, G. L. Fiore, S. J. Rowan and C. Weder, *Nature*, 2011, **472**, 334; (e) J. R. Kumpfer, J. Z. Jin and S. J. Rowan, *J. Mater. Chem.*, 2010, **20**, 145; (f) Y. J. Zhang, T. Han, S. Z. Gu, T. Y. Zhou, C. Z. Zhao, Y. X. Guo, X. Feng, B. Tong, J. Bing, J. B. Shi, J. G. Zhi and Y. P. Dong, *Chem.–Eur. J.*, 2014, **20**, 8856.
- 4 (a) G. F. Manbeck, W. W. Brennessel, R. A. Stockland and R. Eisenberg, *J. Am. Chem. Soc.*, 2010, **132**, 12307; (b) J. Kunzleman, M. Kinami, B. R. Crenshaw, J. D. Protasiewicz and C. Weder, *Adv. Mater.*, 2008, **20**, 119; (c) Y. J. Dong, B. Xu, J. B. Zhang, X. Tan, L. J. Wang, J. L. Chen, H. G. Lv, S. P. Wen, B. Li, L. Ye, B. Zou and W. J. Tian, *Angew. Chem., Int. Ed.*, 2012, **51**, 10782; (d) Y. Wang, M. J. Li, Y. M. Zhang, J. Yang, S. Y. Zhu, L. Sheng, X. D. Wang, B. Yang and S. X. A. Zhang, *Chem. Commun.*, 2013, **49**, 6587; (e) T. Mutai, H. Tomoda, T. Ohkawa, Y. Yabe and K. Araki, *Angew. Chem., Int. Ed.*, 2008, **47**, 9522; (f) Z. Y. Zhang, B. Xu, J. H. Su, L. P. Shen, Y. S. Xie and H. Tian, *Angew. Chem., Int. Ed.*, 2011, **50**, 11654.
- 5 (a) W. Z. Yuan, Y. Q. Tan, Y. Y. Gong, P. Lu, J. W. Y. Lam, X. Y. Shen, C. F. Feng, H. H. Y. Sung, Y. W. Lu, I. D. Williams, J. Z. Sun, Y. M. Zhang and B. Z. Tang, *Adv. Mater.*, 2013, **25**, 2837; (b) Y. Sagara and T. Kato, *Angew. Chem., Int. Ed.*, 2008, **47**, 5175; (c) H. Bi, D. Chen, D. Li, Y. Yuan, D. D. Xia, Z. L. Zhang, H. Y. Zhang and Y. Wang, *Chem. Commun.*, 2011, **47**, 4135; (d) W. E. Lee, C. L. Lee, T. Sakaguchi, M. Fujiki and G. Kwak, *Chem. Commun.*, 2011, **47**, 3526; (e) J. Luo, L. Y. Li, Y. L. Song and J. Pei, *Chem.–Eur. J.*, 2011, **17**, 10515; (f) S. Perruchas, X. F. Le Goff, S. Maron, I. Maurin, F. Guillen, A. Garcia, T. Gacoin and J. P. Boilot, *J. Am. Chem. Soc.*, 2010, **132**, 10967; (g) S. J. Yoon, J. W. Chung, J. Gierschner, K. S. Kim, M. G. Choi, D. Kim and S. Y. Park, *J. Am. Chem. Soc.*, 2010, **132**, 13675; (h) J. Ni, X. Zhang, N. Qiu, Y. H. Wu, L. Y. Zhang, J. Zhang and Z. N. Chen, *Inorg. Chem.*, 2011, **50**, 9090.
- 6 (a) C. Ulbricht, B. Beyer, C. Friebe, A. Winter and U. S. Schubert, *Adv. Mater.*, 2009, **21**, 4418; (b) R. D. Costa, E. Orti, H. J. Bolink, F. Monti, G. Accorsi and N. Armaroli, *Angew. Chem., Int. Ed.*, 2012, **51**, 8178; (c) Y. You and W. Nam, *Chem. Soc. Rev.*, 2012, **41**, 7061; (d) Y. Chi and P. T. Chou, *Chem. Soc. Rev.*, 2010, **39**, 638.
- 7 H. B. Sun, S. J. Liu, W. P. Lin, K. Y. Zhang, W. Lv, X. Huang, F. W. Huo, H. R. Yang, G. Jenkins, Q. Zhao and W. Huang, *Nat. Commun.*, 2014, **5**, 3601.
- 8 E. I. Szerb, A. M. Talarico, I. Aiello, A. Crispini, N. Godbert, D. Pucci, T. Pugliese and M. Ghedini, *Eur. J. Inorg. Chem.*, 2010, 3270.
- 9 (a) G. G. Shan, H. B. Li, H. T. Cao, D. X. Zhu, P. Li, Z. M. Su and Y. Liao, *Chem. Commun.*, 2012, **48**, 2000; (b) G. G. Shan, H. B. Li, D. X. Zhu, Z. M. Su and Y. Liao, *J. Mater. Chem.*, 2012, **22**, 12736.
- 10 (a) N. D. Nguyen, G. Q. Zhang, J. W. Lu, A. E. Sherman and C. L. Fraser, *J. Mater. Chem.*, 2011, **21**, 8409; (b) X. Q. Zhang, Z. G. Chi, B. J. Xu, L. Jiang, X. Zhou, Y. Zhang, S. W. Liu and J. R. Xu, *Chem. Commun.*, 2012, **48**, 10895; (c) Y. L. Wang, W. Liu, L. Y. Bu, J. F. Li, M. Zheng, D. T. Zhang, M. X. Sun, Y. Tao, S. F. Xue and W. J. Yang, *J. Mater. Chem. C*, 2013, **1**, 856; (d) X. G. Gu, J. J. Yao, G. X. Zhang, Y. L. Yan, C. Zhang, Q. Peng, Q. Liao, Y. S. Wu, Z. Z. Xu, Y. S. Zhao, H. B. Fu and D. Q. Zhang, *Adv. Funct. Mater.*, 2012, **22**, 4862.
- 11 (a) G. G. Shan, H. B. Li, H. T. Cao, H. Z. Sun, D. X. Zhu and Z. M. Su, *Dyes Pigm.*, 2013, **99**, 1082; (b) Y. Han, H. T. Cao, H. Z. Sun, Y. Wu, G. G. Shan, Z. M. Su, X. G. Hou and Y. Liao, *J. Mater. Chem. C*, 2014, **2**, 7648.
- 12 E. Orselli, G. S. Kottas, A. E. Konradsson, P. Coppo, R. Frohlich, R. Frtshlich, L. De Cola, A. van Dijken, M. Buchel and H. Borner, *Inorg. Chem.*, 2007, **46**, 11082.
- 13 M. J. Frisch, G. W. Trucks, H. B. Schlegel, G. E. Scuseria, M. A. Robb, J. R. Cheeseman, G. Scalmani, V. Barone, B. Mennucci, G. A. Petersson, H. Nakatsuji, M. Caricato, X. Li, H. P. Hratchian, A. F. Izmaylov, J. Bloino, G. Zheng, J. L. Sonnenberg, M. Hada, M. Ehara, K. Toyota, R. Fukuda, J. Hasegawa, M. Ishida, T. Nakajima, Y. Honda, O. Kitao, H. Nakai, T. Vreven, J. A. Montgomery Jr, J. E. Peralta, F. Ogliaro, M. Bearpark, J. J. Heyd, E. Brothers, K. N. Kudin, V. N. Staroverov, T. Keith, R. Kobayashi, J. Normand, K. Raghavachari, A. Rendell, J. C. Burant, S. S. Iyengar, J. Tomasi, M. Cossi, N. Rega, J. M. Millam, M. Klene, J. E. Knox, J. B. Cross, V. Bakken, C. Adamo, J. Jaramillo, R. Gomperts, R. E. Stratmann, O. Yazyev, A. J. Austin, R. Cammi, C. Pomelli, J. W. Ochterski, R. L. Martin, K. Morokuma, V. G. Zakrzewski, G. A. Voth, P. Salvador, J. J. Dannenberg, S. Dapprich, A. D. Daniels, O. Farkas, J. B. Foresman,

- J. V. Ortiz, J. Cioslowski and D. J. Fox, *Gaussian 09 Revision D.01*, Gaussian, Inc., Wallingford CT, 2013.
- 14 (a) L. He, J. Qiao, L. Duan, G. Dong, D. Zhang, L. Wang and Y. Qiu, *Adv. Funct. Mater.*, 2009, **19**, 2950; (b) C. Rothe, C. J. Chiang, V. Jankus, K. Abdullah, X. S. Zeng, R. Jitchati, A. S. Batsanov, M. R. Bryce and A. P. Monkman, *Adv. Funct. Mater.*, 2009, **19**, 2038; (c) J. D. Slinker, A. A. Gorodetsky, M. S. Lowry, J. Wang, S. Parker, R. Rohl, S. Bernhard and G. G. Malliaras, *J. Am. Chem. Soc.*, 2004, **126**, 2763.
- 15 (a) M. Mydlak, C. Bizzarri, D. Hartmann, W. Sarfert, G. Schmid and L. De Cola, *Adv. Funct. Mater.*, 2010, **20**, 1812; (b) H. C. Su, H. F. Chen, F. C. Fang, C. C. Liu, C. C. Wu, K. T. Wong, Y. H. Liu and S. M. Peng, *J. Am. Chem. Soc.*, 2008, **130**, 3413; (c) T. Sajoto, P. I. Djurovich, A. B. Tamayo, J. Oxgaard, W. A. Goddard and M. E. Thompson, *J. Am. Chem. Soc.*, 2009, **131**, 9813.
- 16 (a) H. Bi, H. Y. Zhang, Y. Zhang, H. Z. Gao, Z. M. Su and Y. Wang, *Adv. Mater.*, 2010, **22**, 1631; (b) J. B. Zhang, J. L. Chen, B. Xu, L. J. Wang, S. Q. Ma, Y. J. Dong, B. Li, L. Ye and W. J. Tian, *Chem. Commun.*, 2013, **49**, 3878.
- 17 (a) F. Ciardelli, G. Ruggeri and A. Pucci, *Chem. Soc. Rev.*, 2013, **42**, 857; (b) G. C. Li, F. J. Song, D. Wu, J. B. Lan, X. Y. Liu, J. Wu, S. J. Yang, D. Xiao and J. S. You, *Adv. Funct. Mater.*, 2014, **24**, 747.
- 18 G. Q. Zhang, J. W. Lu, M. Sabat and C. L. Fraser, *J. Am. Chem. Soc.*, 2010, **132**, 2160.
- 19 (a) M. J. Teng, X. R. Jia, S. Yang, X. F. Chen and Y. Wei, *Adv. Mater.*, 2012, **24**, 1255; (b) P. C. Xue, P. Chen, J. H. Jia, Q. X. Xu, J. B. Sun, B. Q. Yao, Z. Q. Zhang and R. Lu, *Chem. Commun.*, 2014, **50**, 2569; (c) X. Cheng, H. Y. Zhang, K. Q. Ye, H. Y. Zhang and Y. Wang, *J. Mater. Chem. C*, 2013, **1**, 7507.
- 20 (a) Y. Salinas, R. Martinez-Manez, M. D. Marcos, F. Sancenon, A. M. Costero, M. Parra and S. Gil, *Chem. Soc. Rev.*, 2012, **41**, 1261; (b) S. W. Thomas, G. D. Joly and T. M. Swager, *Chem. Rev.*, 2007, **107**, 1339.
- 21 M. E. Germain and M. J. Knapp, *Chem. Soc. Rev.*, 2009, **38**, 2543.
- 22 (a) Y. N. Hong, J. W. Y. Lam and B. Z. Tang, *Chem. Soc. Rev.*, 2011, **40**, 5361; (b) Y. Chen, L. P. Qiao, B. L. Yu, G. Y. Li, C. Y. Liu, L. N. Ji and H. Chao, *Chem. Commun.*, 2013, **49**, 11095; (c) G. G. Shan, H. B. Li, H. Z. Sun, D. X. Zhu, H. T. Cao and Z. M. Su, *J. Mater. Chem. C*, 2013, **1**, 1440; (d) X. G. Hou, Y. Wu, H. T. Cao, H. Z. Sun, H. B. Li, G. G. Shan and Z. M. Su, *Chem. Commun.*, 2014, **50**, 6031.
- 23 (a) S. S. Nagarkar, B. Joarder, A. K. Chaudhari, S. Mukherjee and S. K. Ghosh, *Angew. Chem., Int. Ed.*, 2013, **52**, 2881; (b) G. He, N. Yan, J. Y. Yang, H. Y. Wang, L. P. Ding, S. W. Yin and Y. Fang, *Macromolecules*, 2011, **44**, 4759.
- 24 (a) G. He, H. N. Peng, T. H. Liu, M. N. Yang, Y. Zhang and Y. Fang, *J. Mater. Chem.*, 2009, **19**, 7347; (b) S. Shanmugaraju, S. A. Joshi and P. S. Mukherjee, *J. Mater. Chem.*, 2011, **21**, 9130.
- 25 (a) A. J. Lan, K. H. Li, H. H. Wu, D. H. Olson, T. J. Emge, W. Ki, M. C. Hong and J. Li, *Angew. Chem., Int. Ed.*, 2009, **48**, 2334; (b) N. Dey, S. K. Samanta and S. Bhattacharya, *ACS Appl. Mater. Interfaces*, 2013, **5**, 8394.